Live-cell micromanipulation of a genomic locus reveals interphase chromatin mechanics

Veer I P Keizer, Simon Grosse-Holz, Maxime Woringer, Laura Zambon, Koceila Aizel, Maud Bongaerts, Fanny Delille, Lorena Kolar-Znika, Vittore F Scolari, Sebastian Hoffmann, et al.

Title: **Live-cell micromanipulation of a genomic locus reveals interphase chromatin mechanics**‡‡

Authors: Veer I. P. Keizer[1,2,3,†], Simon Grosse-Holz[1,2,4], Maxime Woringer[1,2], Laura Zambon[1,2,3,‡], Koceila Aizel[2,§], Maud Bongaerts[2], Fanny Delille[5], Lorena Kolar-Znika[1,2], Vittore F. Scolari[1,2], Sebastian Hoffmann[3,¶], Edward J. Banigan[4], Leonid A. Mirny[1,4], Maxime Dahan[2,#], Daniele Fachinetti[3,*], Antoine Coulon[1,2,*,††]

Affiliations:

[1]Institut Curie, PSL Research University, Sorbonne Université, CNRS UMR3664, Laboratoire Dynamique du Noyau, 75005 Paris, France.

[2]Institut Curie, PSL Research University, Sorbonne Université, CNRS UMR168, Laboratoire Physico Chimie Curie, 75005 Paris, France.

[3]Institut Curie, PSL Research University, CNRS UMR144, Laboratoire Biologie Cellulaire et Cancer, 75005 Paris, France.

[4]Department of Physics and Institute for Medical Engineering and Science, Massachusetts Institute of Technology, Cambridge, 02139 MA, USA.

[5]ESPCI Paris, PSL Research University, Sorbonne Université, CNRS UMR8213, Laboratoire de Physique et d'Étude des Matériaux, 75005 Paris, France.

[†]Present address: National Cancer Institute, NIH, Bethesda, MD, USA.

[‡]Present address: Lifeanalytics srl, Oderzo, Veneto, Italy.

[§]Present address: TreeFrog Therapeutics, Pessac, France.

[¶]Present address: Boehringer Ingelheim Pharma GmbH & Co. KG, Biberach an der Riss, Germany.

[#]Deceased.

[*]Correspondence: daniele.fachinetti@curie.fr, antoine.coulon@curie.fr

[††]Lead contact.

‡‡ This manuscript has been accepted for publication in *Science*. This version is the *Author Accepted Manuscript* (AAM) and has not undergone final editing. Please refer to the *Final Published Version* (FPV) at https://www.science.org/doi/10.1126/science.abi9810. The FPV manuscript may not be reproduced or used in any manner that does not fall within the fair use provisions of the Copyright Act without the prior, written permission of AAAS. This research was funded in part by cOAlition S organizations. Hence, the AAM version (this document) is available under CC BY 4.0 license.

Abstract: Our understanding of the physical principles organizing the genome in the nucleus is limited by the lack of tools to directly exert and measure forces on interphase chromosomes *in vivo* and probe their material nature. Here, we introduce an approach to actively manipulate a genomic locus using controlled magnetic forces inside the nucleus of a living human cell. We observe viscoelastic displacements over microns within minutes in response to near-picoNewton forces, which are consistent with a Rouse polymer model. Our results highlight the fluidity of chromatin, with a moderate contribution of the surrounding material, revealing minor roles for crosslinks and topological effects, and challenging the view that interphase chromatin is a gel-like material. Our technology opens avenues for future research, from chromosome mechanics to genome functions.

One-Sentence Summary: An approach for probing the force response of interphase chromosomes in living cells reveals their material nature.

Main Text:

Recent progress in observing and perturbing chromosome conformation has led to an unprecedented understanding of the physical principles at play in shaping the genome in 4 dimensions (4D) (*1*). From genomic loops and topologically associating domains (TADs) to spatially segregated A/B compartments and chromosome territories, the different levels of organization of the eukaryotic genome are thought to arise from various physical phenomena, including phase separation (*2–4*), ATP-dependent motors (*4*, *5*), and polymer topological effects (*6*). Nonetheless, the physical nature of chromatin and chromosomes inside the nucleus and its functional implications for mechanotransduction remain an active area of investigation (*7*, *8*). Observation-based studies assessing the mobility of the genome in living cells, from single loci (*9–11*) and small regions (*12*) to large domains (*13*), underline the possible existence of different material states of chromatin (liquid, solid, gel-like). Extra-nuclear mechanical perturbations, including whole-nucleus stretching (*14*, *15*), micro-pipette aspiration (*16*), and application of local pressures (*16*, *17*) or torques (*18*) onto a cell, all affect the overall geometry of the nucleus and reveal global viscoelastic properties. Intra-nuclear mechanical manipulation of the genome, on the other hand, is rare and technically challenging (*8*). Viscoelasticity measurements using a microinjected 1 μm bead suggested that interphase chromatin may be a crosslinked polymer network (i.e. gel) (*19*). Recently, intra-nuclear mechanics was elegantly probed by monitoring the fusion of both artificial (*20*) and naturally-occurring (*21*) droplet-like structures. Active mechanical manipulation of an intra-nuclear structure was recently achieved using an optical tweezer to displace a whole nucleolus in oocytes (*22*) and using optically induced thermophoretic flows within prophase (*23*) or interphase nuclei (*24*). However, these approaches are limited to the manipulation of large structures or do not apply forces directly on chromatin. These limitations have made it difficult to disentangle various effects (mechanical response of the nucleus *vs*. chromatin itself; hydrodynamics *vs.* polymer viscoelasticity), leading to contradictory results. Hence, an approach for the direct and active mechanical manipulation of specific genomic loci inside living cells is needed. To meet this need, we developed a technique for targeted micro-manipulation of a specific genomic locus in the nucleus of a living cell, allowing us to probe the physical properties of an interphase chromosome by measuring its response to a controlled point force.

Results

Mechanical manipulation of a genomic locus in a living cell

Our approach relies on tethering magnetic nanoparticles (MNPs) to a genomic locus and applying an external magnetic field (Fig. 1A). We chose ferritin MNPs for their small size (*25*, *26*): 12 nm in diameter for ferritin (PDB 1GWG), 28 nm for the full MNP (*26*). We produced ferritin MNPs by synthesizing *in vitro* recombinant eGFP-labeled ferritin cages and loading them with a magnetic core (see *Methods*). We microinjected MNPs into the nuclei of living human U-2 OS cells previously engineered to contain an artificial array inserted at a single genomic location in a subtelomeric region of chromosome 1 (band 1p36) (*27*). This genomic array contains ~200 copies of a 20 kb genetic construct, each including 96 *tetO* binding sites and a transgene. It has been extensively used in the past to study the function of several chromatin modifications, RNA polymerase II (Pol II) recruitment, and RNA synthesis during induction of the transgene (*27–29*). Hence, although we used it here uninduced, this array can recapitulate functional chromatin-based processes, such as transcriptional activation. MNPs were targeted to the array using a constitutively expressed fusion protein (TetR, mCherry and anti-GFP nanobody) serving as a tether (Fig 1A). Upon injection, MNPs diffused through the nucleus and accumulated at the array, forming a fluorescent spot in both eGFP and mCherry channels (fig. S1A and fig. S2A). Quantification of the fluorescence signals indicated that MNPs were at nanomolar concentrations in the nucleus following injection and accumulated at the genomic locus in the range of hundreds to thousands of MNPs (median 1500 MNPs; see fig. S1B, fig. S3, movie S1, table S1 and *Methods*). The locus should be regarded as a condensed and heterochromatic 4 Mb region (1.6% of chromosome 1) residing in a euchromatic genomic context, as previously reported (*27*), with small MNPs (each being ~2-3 times (*26*) the size of a nucleosome) sparsely decorating chromatin (1 MNP per ~2.7kb). Consistently, we observed that the locus typically resided in low to intermediate DNA density regions and is itself relatively condensed (fig. S4A-B) and that binding of MNPs to the locus did not substantially affect its morphology (fig. S2A-B). Microinjection and attraction of unbound MNPs did not substantially alter chromatin distribution and densities inside the nucleus (as assessed by SiR-DNA staining; fig. S2C-D). Cells were imaged on a coverglass with custom-made microfabricated pillars (*30*, *31*), which behave as local magnets only when subjected to an external magnetizing field (fig. S5). Hence, ON/OFF modulation of the local force field could be achieved while imaging by placing/removing an external magnet on the microscope stage. The shape and orientation of the pillars were chosen to maximize the magnetic field gradient and hence the force. We performed magnetic simulations and experimental calibrations using two independent methods (see *Methods*; fig. S6, fig. S7 and movie S2) to determine the magnitude and orientation of the force applied onto the genomic locus, as a function of the number of MNPs bound to it and its position relative to the magnetic pillar (Fig. 1B). The typical forces applied onto the locus were in the sub-picoNewton (pN) range, occasionally reaching a few pN (table S1; median force = 0.45 pN). These values are in the range of forces exerted by molecular motors in the nucleus, e.g. comparable to the stalling force of ~0.5 pN for the structural maintenance of chromosomes (SMC) complex condensin (*32*) and a few pN for RNA polymerase II (Pol II) (*33*).

Force-induced movement of a genomic locus reveals viscoelastic properties of chromatin

We first applied the magnetic force for 30 min and released it for another 30 min, while performing low-illumination 3D imaging with a 2 min interval (30'-PR scheme). We observed a clear motion of the locus toward the magnet upon application of the force and a slow and partial recoil when the force stopped (Fig. 1C-D, movie S3). This indicates that a sub-pN force, when applied in a

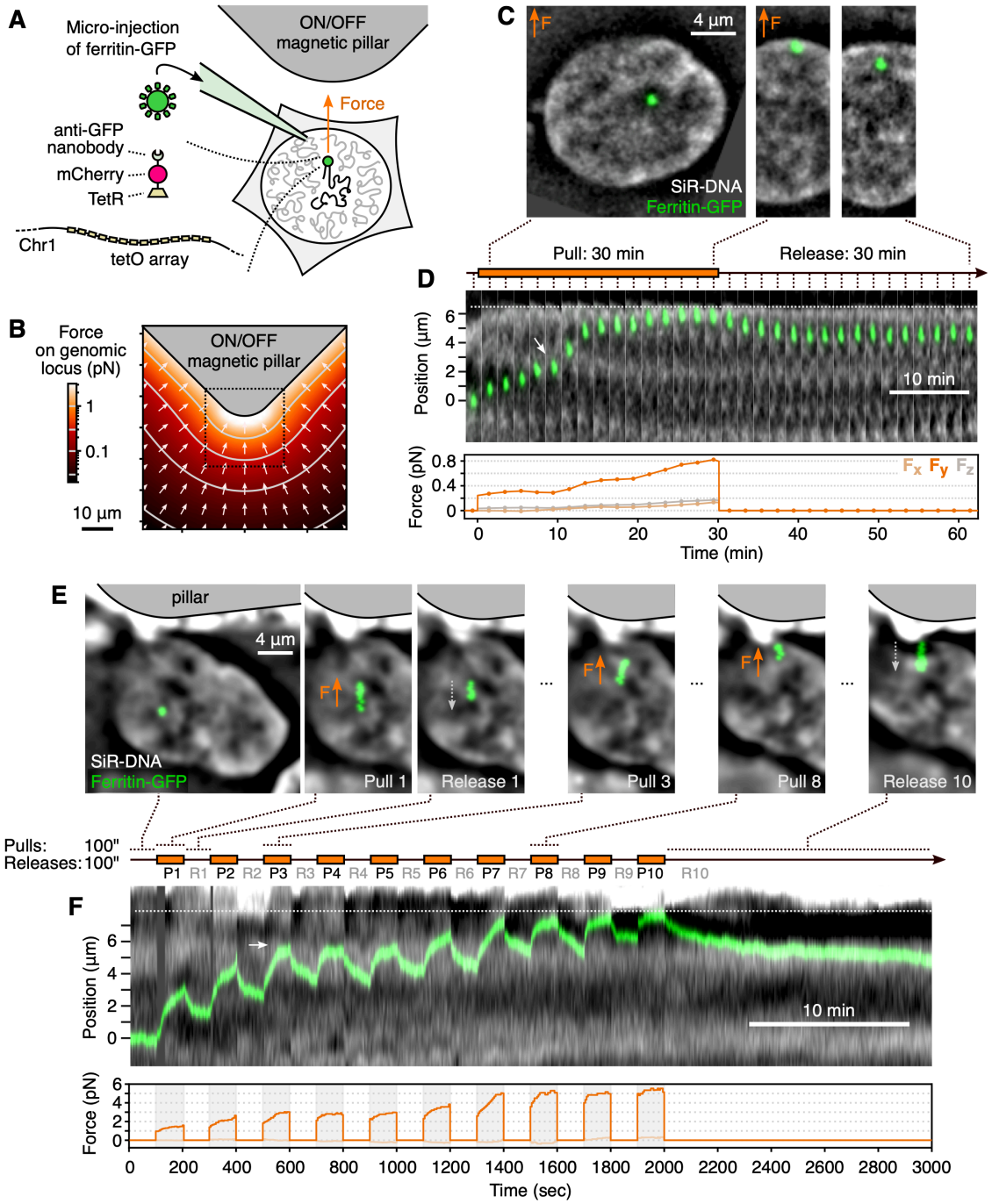

Fig. 1. **Mechanical micro-manipulation of a genomic locus in living cells.** (**A**) Magnetic nanoparticles (MNPs) of GFP-labeled ferritin are microinjected into the cell nucleus and targeted to a genomic array containing ~19,000 tetO binding sites (*27*) with a linker protein. Cells are imaged on a coverslide with microfabricated magnetic pillars that produce a local magnetic field and attract the genomic locus. (**B**) The force exerted onto the locus depends on its position relative to the pillar and is characterized using a pre-calculated force map (see *Methods*), here shown for 1000 MNPs at the locus. (**C**) Example of a pull-release experiment showing the locus being displaced during the 30 min of force exertion and recoiling during the 30 min of force release (30'-PR scheme). See also movie S3. (**D**) Kymograph of the same experiment showing each time frame, along with the force time profile calculated using the force map. (**E**) Experiment where pulls and releases are 100 sec and the pull-release cycle is repeated 10× (100"-PR scheme). Images are time projections, i.e. showing in green all the positions of the center of mass of the locus over the periods represented on the timeline. The arrows indicate the direction of the motion. See also movie S4. (**F**) Kymograph of the same experiment, showing the displacement of the locus and the spatial patterns of DNA density in the nucleus, along with the force time profile. All SiR-DNA images are band-passed (see *Methods*). On (D, F), dotted lines: nuclear periphery, white arrows: feature of interest in the spatial distribution of DNA density.

sustained and unidirectional manner on a genomic locus, elicits a displacement of that locus by several microns over minutes. It also shows that the chromosomal locus can move across the nuclear environment, which is believed to be crowded and entangled. We also applied the force periodically –pulling for 100 sec, releasing for 100 sec and repeating this cycle 10 times (100"-PR scheme)– while performing fast 2D imaging with a 5 sec interval (Fig. 1E-F, movie S4). Several observations from these two experiments hinted at the material properties of chromatin. First, the trajectories showed recoils during release periods and a gradual slow-down during both pulls and releases, characteristic of a viscoelastic material. Second, spatial heterogeneities in the trajectories were visible and appeared to relate to the spatial distribution of DNA density (Fig. 1D and F; white arrows; the motion of the locus was hindered where the DNA density varied). Third, recoil after force release was seen even after collision with the nuclear periphery, indicating that the material there (peripheral heterochromatin, nuclear lamina) was not sticky enough to fully retain the locus. Fourth, the spatial distribution of DNA density in the nucleus does not show large-scale deformations, indicating that the locus did not drag along large amounts of material (movie S3 and movie S4). Together, the force-induced displacements we observed are consistent with viscoelastic and non-confining chromatin and constitute a basis to further develop and test physical models of interphase chromosomes.

Quantitative force-response and scaling laws of interphase chromatin mechanics

To quantify viscoelastic properties of chromatin, we analyzed the trajectories of the locus in 35 cells undergoing the 30'-PR scheme (corrected for cell motion and force orientation, see *Methods*). We observed a range of behaviors in both pulls and releases, regarding initial speed, total distance travelled, and shape of time profiles (Fig. 2A-B and fig. S8). Most traces showed a displacement that was clearly distinguishable from diffusion (Fig. 2A-B, hatched areas; see *Methods*). Collision with the nuclear periphery (open symbols on Fig. 2A-B and fig. S8) happened in 9 out of 35 traces and hence the total displacement during the pull is most often not limited by the nuclear periphery. The initial force applied onto the locus largely predicted the variability seen in the initial motion (Fig. 2C and fig. S9A). The recoil motion after force release was in part predicted by the total distance over which the locus had been displaced during the pull (Fig. 2D and fig. S9B), with a simple linear relationship highlighting the elastic nature of chromatin. Deviations from these simple proportionality relationships indicate that the specific nuclear context or the state of the genomic locus might influence its response. In particular, we observed that when the locus moved slower than expected, it was less DNA dense, and when the locus moved faster than expected, it was more DNA dense (fig. S4C), suggesting that the compaction state of the locus itself affected its response to the force. Absolute nuclear position of the locus did not correlate with its response to the force, but if the locus reached the periphery during the pull, it often recoiled slower than expected (fig. S10). Despite the variability between traces, log-log plots of all the pulls and releases from the 30'-PR and 100"-PR trajectories, together with 3 additional high-framerate (dt = 0.5") pull-release trajectories, revealed linear portions in the curves with a slope of 0.5, over more than three orders of magnitude in time (Fig. 2E). This behavior suggests that the different levels of the hierarchical genome organization are not characterized by vastly distinct mechanical properties. In addition, displacements that scale with time as $t^{1/2}$ can be empirically described by a 'fractional speed', i.e., a single value in $\mu m/s^{1/2}$ capturing how the motion evolves over time (Fig. 2C-D and fig. S9, right axes). The first pull of the 100"-PR trace, represented in this unit, indeed follows the same relationship as the 30'-PR traces (dark green triangle on Fig. 2C) and the slope of the resulting force-displacement plot yields a unique factor of 0.158 (± 0.014) $\mu m/s^{1/2}/pN$, characterizing the dynamic response of chromatin to force. Together, these results indicate that a large part of the response of chromatin to force can be described by simple laws.

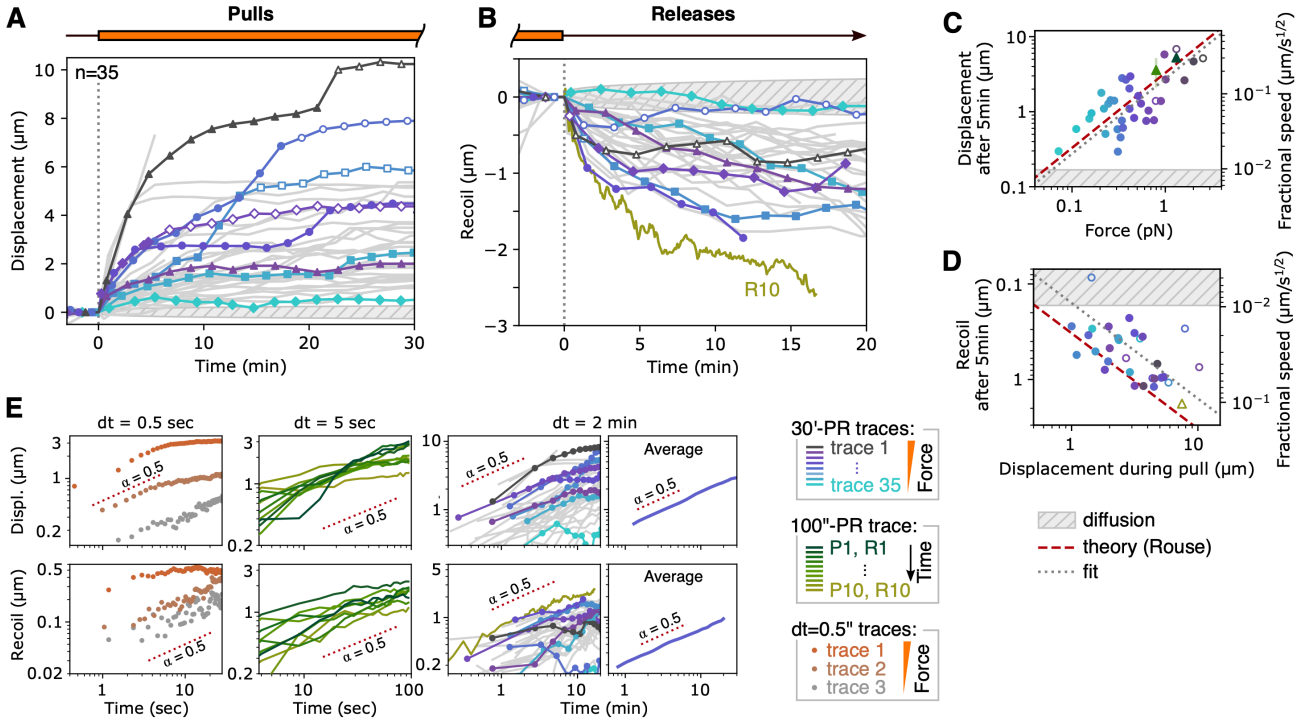

Fig. 2. **Quantitative analysis of locus movement in response to force**. (**A**) Trajectories of the genomic locus in the direction of the applied force for 35 different cells during force exertion with the 30'-PR scheme. A selection of trajectories, representative of the breadth of observed behaviors, are highlighted and color-coded by force (See fig. S8 for individual trajectories). Hatched areas in A to D correspond to the null model of pure diffusion based on MSD measurement (see *Methods*). (**B**) Recoil trajectories relative to the time and position at the start of the release are shown for the same loci as in A. Curve R10 is the last release of the 100"-PR trajectory. (**C**) Displacements measured at $\Delta t = 5$ min of force exertion on all the traces from A, plotted against the magnitude of the force. Coordinates are interpolated between the frames before/after Δt. The green line/triangle correspond to the envelope of the 100"-PR trajectory. Reported forces are the average over Δt. Displacements are also expressed in $\mu m/s^{1/2}$ (right axis), allowing us to place pull P1 from the 100"-PR trace, measured at $\Delta t = 100s$ (dark green triangle). The red line indicates the expected relationship from Rouse theory, solely based on an MSD measurement. (**D**) Recoil after $\Delta t = 5$ min of force release on all the traces from B and the last release of the 100"-PR trajectory (R10, green triangle), plotted against the total displacement during the pull. The red line indicates the expected relationship from Rouse theory. (See fig. S9 for versions of C and D at different Δt and in linear scales). Open symbols on A-D indicate when loci are within 1.5 μm of the nuclear periphery (at the moment of measurement on A-C, at the moment of force release on D). (**E**) Displacement and recoil trajectories, aligned on the time and position at the moment of force switching, are represented as log-log plots for pull-release experiments imaged with different frame intervals: dt = 0.5 sec (see *Methods*), dt = 5 sec (from the 100"-PR trace; Fig. 1F), and dt = 2min (all 30'-PR traces; panels A and B). For the latter, average trajectories (right plots) were calculated over all displacements where the applied force remains ≤ 2 pN (28/35 traces) and over all the recoils after a displacement of ≤ 5 μm (21/35 traces). Red dotted lines indicate the power-law behavior, with exponent 0.5, predicted by Rouse theory.

Chromatin force response is well described by a free polymer model (Rouse chain)

We then sought a model of chromatin that best explains our quantitative measurement of force-induced locus displacement. Several features in our data suggest a classical polymer model known as a *Rouse* polymer (*34*) as a first approximation to describe the response of chromatin to forces. The Rouse model represents a polymer in which each monomer diffuses by thermal motion in a viscous medium and is connected to its two neighbors by elastic bonds. Importantly, Rouse ignores steric effects (contact, hindrance), crosslinks (affinity, stickiness), and topological effects (fibers can pass through each other). This model is frequently invoked for chromatin dynamics since it predicts the characteristic power-law scaling –i.e. a linear relationship on a log-log plot– of the

mean squared displacement (MSD) *vs.* time, with exponent 0.5, as observed here (fig. S11A and E) and for other genomic loci in eukaryotes (*35–37*). We extended Rouse theory to study how a polymer responds to a point force (see *Methods* and Supplementary Text). Our calculations predict a power-law behavior with exponent 0.5 for displacements and recoils in response to force, consistent with our experimental observations (Fig. 2E). These two power laws have the same physical origin, so the diffusion coefficient obtained independently from the MSD ($1{,}627 \pm 19$ nm^2.s$^{-1/2}$, fig. S11A) directly relates to –and predicts– the slope of the force-displacement plot (Fig. 2C, red line), i.e. $1{,}627$ nm^2.s$^{-1/2}$ / $2k_BT = 0.190 \pm 0.003$ µm/s$^{1/2}$/pN; see *Methods*. This agreement between two independent passive and active measurements (diffusion and force response, i.e. red *vs.* gray lines on Fig. 2C and fig. S9A) supports the Rouse model to explain our chromatin dynamics data. Inspected on a cell-by-cell basis, the force-free MSD of the locus before and after the pull-release experiments appears very moderately reduced in most cases (fig. S11B). Its natural variability between cells does not appear to explain the variability of the response to force (fig. S11C). After force release, the Rouse model also predicts a recoil proportional to the total displacement during the pull. However, in many cases, the locus recoiled somewhat slower than predicted by the Rouse theory. Instead, the theoretical prediction appears to define an upper bound for the recoils (Fig. 2D and fig. S9B, red lines) and deviations from Rouse theory are more pronounced at the nuclear periphery (fig. S10B). Together, this analysis suggests that the dynamic response of the chromosome to the force can be described by the Rouse polymer model, with additional effects from the nuclear environment.

Model-based trajectory analysis reveals moderate hindrance by surrounding chromatin

To further understand the physical nature of chromatin, we asked how alternative polymer models are able to capture the 100”-PR trace (Fig. 3A-D). The approach is to use the displacement trajectory and infer, assuming a given polymer model, the time profile of the force that produced the measured trajectory (see *Methods*, Supplementary Text and fig. S12A-C). Disagreement between predicted and actual force profiles indicates when models are incorrect or incomplete, allowing one to select and refine the best model(s). With this approach, we compared a series of models (fig. S12C). First, a simple Rouse model without any adjustable parameters (i.e. calibrated using the MSD *vs.* time plot; fig. S11A) predicts well the first pull and all the release periods (Fig. 3B). However, the prediction leaves some of the applied force unexplained (gray area between curves, Fig. 3B), suggesting a missing component in the model that would additionally slow down or hinder the progression of the locus. This residual unexplained force did not scale with speed and hence could not be explained as an additional viscous drag on the locus (fig. S12D). Instead, it increased progressively across successive pulls, suggesting an accumulation of hindrance as the locus moved through the nucleus. To represent this, we added a capacity for the locus to interact with the surrounding chromatin, represented as extra Rouse chains that are either attached to or pushed by the locus along its path (Fig. 3C and fig. S12C). These models better predicted the force profile throughout the trajectory compared to a pure Rouse model. The only free parameter in Fig. 3C is the frequency at which the locus interacts with other polymers, which we found very low (fig. S12C), indicating that the interaction with the surrounding chromatin was moderate. This is also consistent with the small but detectable reduction in mobility of the locus before and after pull-release experiments (fig. S11B) and the subtle redistribution of DNA densities around the pulled locus (fig. S4D). Taken together, these modeling results suggest that, upon force application and release on our genomic locus, chromatin is well described as a Rouse polymer –i.e. a free polymer in a viscous environment– with moderate interactions from the surrounding chromatin, indicating that hindrance, crosslinks, and topological effects play a minor role.

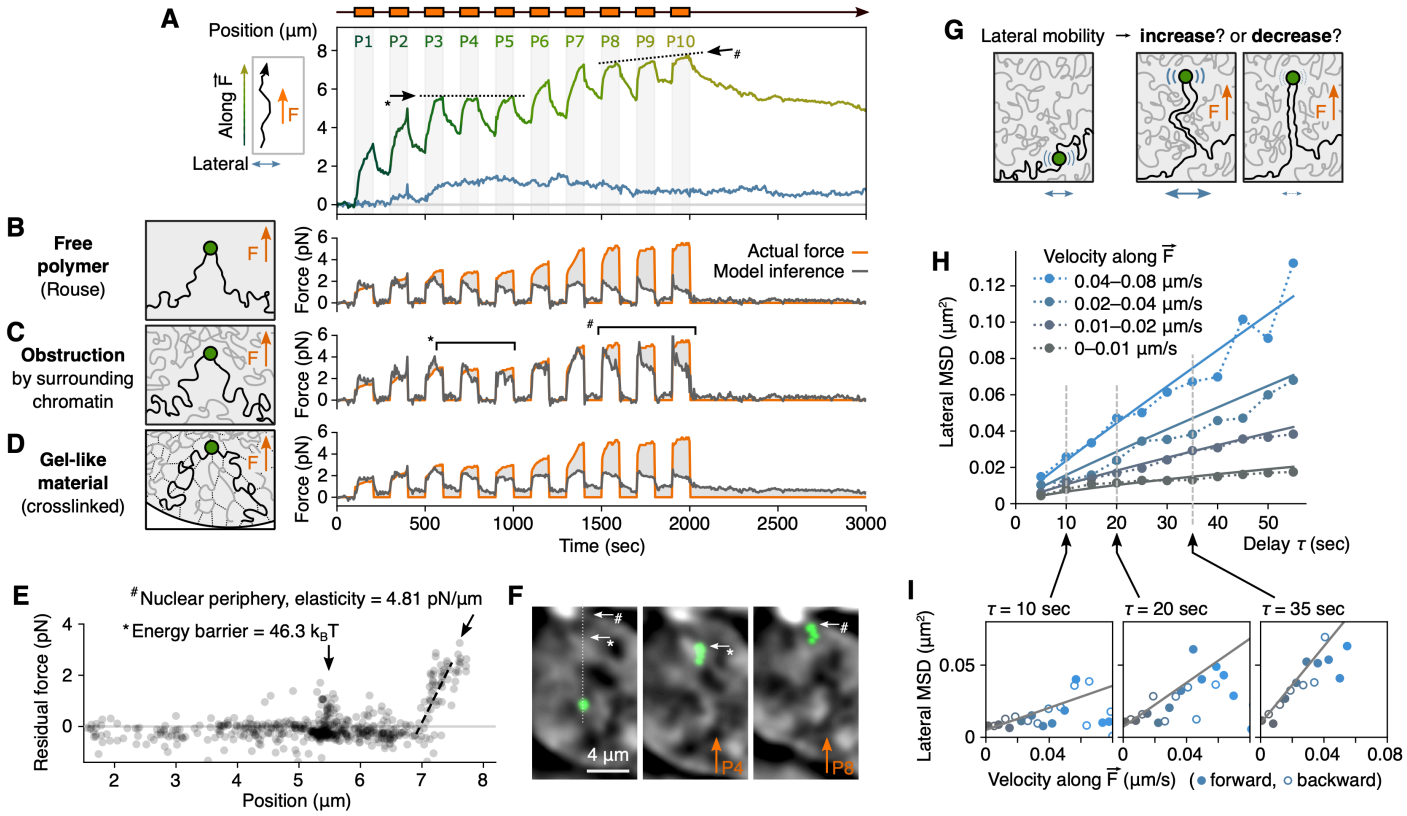

Fig. 3. **Model-based analysis and hypothesis testing.** (**A**) Trajectory of the locus shown in the direction of the force (green curve) and orthogonal to the force in the imaging plane (blue curve) for the 100”-PR experiment. Arrows indicate apparent obstacle (see also * and # in panels C, E and F). (**B-D**) Evaluation of different models in their capacity to reproduce the experimentally measured force time profile (orange curve) by inferring it from the trajectory (gray curve). Models shown here are (**B**) a simple Rouse polymer (*34*), (**C**) the same model with extra polymer chains being pushed by the locus to represent the surrounding chromatin, and (**D**) a gel-like material, represented as a Rouse polymer in a viscoelastic environment. See full list in fig. S12. (**E**) The residual unexplained force from the second model (area between curves in C) is plotted along the trajectory of the locus, highlighting an obstacle (*) and an elastic region near the nuclear periphery (#) for which physical parameters are measured (see *Methods*) and which are visible in panels A, C and F. (**F**) Time projection images, respectively before the first pull and during pulls P4 and P8, showing how the spatial distribution of DNA density in the nucleus relates to the identified obstacles. SiR-DNA images are band-passed (see *Methods*). (**G**) Hypotheses on how the lateral mobility of the locus may change depending on its force-induced displacement. (**H-I**) Mean square displacement (MSD) of the lateral movement of the locus, calculated as a function of both time delay and velocity in the direction of the force. Solid lines on both the MSD-delay (H) and the MSD-velocity (I) representations correspond to a single-parameter fit describing how lateral mobility increase with velocity in the direction of the force.

Interphase chromatin does not behave as a gel in force-response experiments

Interphase chromatin was proposed to be a gel-like material (*11*, *12*, *19*). A gel is a highly crosslinked polymer, i.e. unlike a linear polymer where monomers are linked to two neighbors, extra links between non-adjacent monomers form an interconnected mesh, giving the gel solid-like properties. For chromatin, this could in principle arise from affinity between nucleosomes, as well as loops/bridges formed by proteins/complexes/condensates and topological entanglement between chromatin fibers. First, in such an interconnected mesh structure, short paths effectively linking the pulled locus to all other loci in the nucleus would result in long-range deformation of the spatial pattern of DNA density, which we do not observe (Fig. 1D,F, movie S3 and movie S4). Second, if the chromatin surrounding the locus were gel-like, it would effectively act as a viscoelastic medium. This assumption does not recapitulate well the experimental data (even with two free parameters, Fig. 3D and fig. S12C) and is inconsistent with the observed scaling of 0.5 in

the MSD (fig. S11A and E), which argues for a simply viscous and non-elastic medium. Finally, if the locus was part of an interconnected mesh, short series of links would tether it to large structures (e.g. periphery, nucleoli). A Rouse model that includes a finite tether does not recapitulate the experimental data (fig. S12C) and is inconsistent with the linear behavior observed in Fig. 2E up to several microns. These results again suggest again minor effects of crosslinks and topological constraints and argue against the view that interphase chromatin behaves like a gel at the spatial and temporal scale of our observations.

Heterogeneities in the trajectory reveal obstacles in the nuclear interior and a soft elastic material at the nuclear periphery

Even the models that best capture the data leave part of the force unexplained (Fig. 3C, gray area). We thus plotted this residual unexplained force as a function of spatial position (Fig. 3E). This revealed an accumulation of non-null residual forces at specific locations, matching visible features in the trajectory and in spatial distribution of DNA density in the nucleus. First, the residual force in pulls P3 to P5 corresponds to an apparent obstacle in the trajectory (* on Fig. 3A,C) occurring at a high-to-low transition of DNA density (Fig. 3F and Fig. 1F). It appears as a spatially defined barrier of residual force (Fig. 3E), requiring an energy of ≈46 k_BT to overcome. This suggests that, while DNA dense regions are not obstacles *per se*, the interface between high- and low-density regions may constitute a barrier. The energy we estimated suggests that such barriers may be overcome by ATP-dependent molecular motors (*32*, *33*) but unlikely by spontaneous thermal fluctuations. Second, the residual force in pulls P8 to P10 (# on Fig. 3A,C) corresponds to the collision with structures near the nuclear periphery (Fig. 1F and # on Fig. 3F). The observed linear force-distance relationship (Fig. 3E) indicates a solid-like elastic behavior for these structures, over at least 600 nm and with a spring constant of 4.81 pN/µm. This is much softer than what was measured by whole-nucleus stretching experiments (*14*, *15*), which could be explained by the small size of the locus and/or the existence of a soft layer of elastic peripheral components (heterochromatin, nuclear lamina) rather than the material directly contributing to the structural rigidity of the nucleus.

Lateral mobility of the locus reflects transient collisions with obstacles in the nucleoplasm

To further investigate the material encountered by the locus, we analyzed the lateral motion of the locus as it was pulled and released (Fig. 3A, blue curve). We hypothesized that, on one hand, collisions with obstacles could increase lateral mobility or, on the other hand, the locus being dragged into a more constraining and entangled environment could result in a reduction of its mobility (Fig. 3G). After computing the MSD of the lateral motion as a function of both time delay τ and velocity v_y along the direction of the force (Fig. 3H-I and fig. S11F-G), we observed a clear increase of lateral mobility when the locus moved (for both forward and backward movements; Fig. 3I), suggesting the existence of obstacles that deflected the motion. This additional mobility in the MSD is captured by a term proportional to v_y, as expected for collisions, and proportional to τ (not $\tau^{0.5}$), as expected if the force due to the collision with obstacles persists in the same direction across several frames, indicating the existence of large obstacles. Indeed, in P3 for instance, the lateral motion clearly shows a directional behavior (Fig. 1E and Fig. 3A). However, the relationships we observed on Fig. 3H-I held even when excluding all the timepoints before P4 (fig. S11H-I), indicating that the collision with obstacles was widespread throughout the nucleus. These results, together with our observation that very few chromatin fibers appeared to be carried along with the locus, indicate that obstacles are frequently encountered by the locus, but most interactions are weak and transient.

Discussion

Our measurements of how a genomic locus inside the nucleus of a living cell responds to a point force indicates that interphase chromatin has fluid-like properties and behaves as a free polymer. This contrasts with previous studies depicting chromatin as a stiff, crosslinked polymer gel with solid-like properties (*11*, *12*, *19*). Our observation that near-pN forces can easily move a genomic locus across the nucleus over a few minutes (Fig. 1D,F) also contrasts with a previous study reporting confined sub-micron displacements over seconds upon application of 65 to 110 pN forces to a 1-µm bead (*19*). We propose that our results may be reconciled with previous experiments in several ways. First, unlike a micron-size bead, the locus in our experiments is small and may be deformable enough to pass through the surrounding chromatin. Second, chromatin may contain many small, gel-like patches, embedded in a structure with liquid, Rouse-like properties at a larger scale. This is also in line with our observation that the transiting locus frequently encounters obstacles. Third, chromatin may be a *weak gel*, i.e. with short-lived crosslinks (*11*). Such a gel could continuously maintain a stiff, globally connected network that resists stresses over large length scales, while permitting fluid-like motions at smaller scales. Future experiments perturbing chromatin state and chromatin associated proteins will be important to reconcile observed micro- and mesoscale mechanics.

Organization of chromosomes that allows movement of genomic loci across large distances by weak forces could have implications for a range of genome functions. Large-scale movements of chromosomes occur during nuclear inversion in rod cell differentiation for nocturnal mammals (*38*). Specific genes undergo long-range directional motion upon transcriptional activation (*39*, *40*). Long and highly transcribed genes can form ~5 µm giant loops, believed to be due to chromosome fiber stiffening (*41*). Certain double strand break sites undergo large-scale, nuclear F-actin dependent relocation to the nuclear periphery (*42*). These DNA-based biological processes require a nuclear organization in which such movements are possible. Our results reveal mechanical properties of chromatin where such large-scale movements would only require weak (near pN) forces. Although sustained unidirectional forces are unlikely to occur naturally in the nucleus, the magnitude of the forces and the timescale of force exertion in our experiments are comparable to those of molecular motors like SMC complexes and Pol II –i.e. in the sub-pN (*32*) or low-pN (*33*) ranges and applied over minutes (e.g. 10 min for Pol II to elongate through a 25kb gene, 5-30 min for SMC complexes). Hence, some molecular motors in the nucleus operate in a force range that is sufficient to substantially reorganize the genome in space.

Future work will be important to expand and complement our results. Although the genomic array we used here is known to be chromatinized and has been used extensively to recapitulate and study functional chromatin-based processes (*27–29*), we cannot exclude that its repetitive and artificial nature might prevent some of our measurements from being applicable to non-repetitive and native regions. Manipulating loci other than a subtelomeric locus on the longest chromosome (chromosome 1), in other genomic contexts (hetero-/euchromatin), and in different cell types will be important to assess the generalizability of our findings in various biological contexts.

Our approach to mechanically manipulate and relocate genomic loci in the nuclear space opens many avenues for future research, from the study of interphase chromosome mechanics to the perturbation of genome functions, including transcription, replication, DNA damage repair and chromosome segregation. By giving access to physical parameters and revealing fundamental scaling laws to describe chromatin mechanics, our work provides a foundation for future theories of genome organization.

References and Notes

1. the 4D Nucleome Network, J. Dekker, A. S. Belmont, M. Guttman, V. O. Leshyk, J. T. Lis, S. Lomvardas, L. A. Mirny, C. C. O'Shea, P. J. Park, B. Ren, J. C. R. Politz, J. Shendure, S. Zhong, The 4D nucleome project. *Nature*. **549**, 219–226 (2017).
2. D. Jost, P. Carrivain, G. Cavalli, C. Vaillant, Modeling epigenome folding: formation and dynamics of topologically associated chromatin domains. *Nucleic Acids Research*. **42**, 9553–9561 (2014).
3. D. Hnisz, K. Shrinivas, R. A. Young, A. K. Chakraborty, P. A. Sharp, A Phase Separation Model for Transcriptional Control. *Cell*. **169**, 13–23 (2017).
4. L. A. Mirny, M. Imakaev, N. Abdennur, Two major mechanisms of chromosome organization. *Current Opinion in Cell Biology*. **58**, 142–152 (2019).
5. E. J. Banigan, L. A. Mirny, Loop extrusion: theory meets single-molecule experiments. *Current Opinion in Cell Biology*. **64**, 124–138 (2020).
6. J. D. Halverson, J. Smrek, K. Kremer, A. Y. Grosberg, From a melt of rings to chromosome territories: the role of topological constraints in genome folding. *Rep. Prog. Phys.* **77**, 022601 (2014).
7. C. Uhler, G. V. Shivashankar, Regulation of genome organization and gene expression by nuclear mechanotransduction. *Nat Rev Mol Cell Biol*. **18**, 717–727 (2017).
8. A. A. Agbleke, A. Amitai, J. D. Buenrostro, A. Chakrabarti, L. Chu, A. S. Hansen, K. M. Koenig, A. S. Labade, S. Liu, T. Nozaki, S. Ovchinnikov, A. Seeber, H. A. Shaban, J.-H. Spille, A. D. Stephens, J.-H. Su, D. Wadduwage, Advances in Chromatin and Chromosome Research: Perspectives from Multiple Fields. *Molecular Cell*. **79**, 881–901 (2020).
9. T. Nozaki, R. Imai, M. Tanbo, R. Nagashima, S. Tamura, T. Tani, Y. Joti, M. Tomita, K. Hibino, M. T. Kanemaki, K. S. Wendt, Y. Okada, T. Nagai, K. Maeshima, Dynamic Organization of Chromatin Domains Revealed by Super-Resolution Live-Cell Imaging. *Molecular Cell*. **67**, 282-293.e7 (2017).
10. B. Chen, L. A. Gilbert, B. A. Cimini, J. Schnitzbauer, W. Zhang, G.-W. Li, J. Park, E. H. Blackburn, J. S. Weissman, L. S. Qi, B. Huang, Dynamic Imaging of Genomic Loci in Living Human Cells by an Optimized CRISPR/Cas System. *Cell*. **155**, 1479–1491 (2013).
11. N. Khanna, Y. Zhang, J. S. Lucas, O. K. Dudko, C. Murre, Chromosome dynamics near the sol-gel phase transition dictate the timing of remote genomic interactions. *Nat Commun*. **10**, 2771 (2019).
12. H. Strickfaden, T. O. Tolsma, A. Sharma, D. A. Underhill, J. C. Hansen, M. J. Hendzel, Condensed Chromatin Behaves like a Solid on the Mesoscale In Vitro and in Living Cells. *Cell*. **183**, 1772-1784.e13 (2020).
13. A. Zidovska, D. A. Weitz, T. J. Mitchison, Micron-scale coherence in interphase chromatin dynamics. *Proceedings of the National Academy of Sciences*. **110**, 15555–15560 (2013).
14. A. D. Stephens, E. J. Banigan, S. A. Adam, R. D. Goldman, J. F. Marko, Chromatin and lamin A determine two different mechanical response regimes of the cell nucleus. *MBoC*. **28**, 1984–1996 (2017).
15. Y. Shimamoto, S. Tamura, H. Masumoto, K. Maeshima, Nucleosome–nucleosome interactions via histone tails and linker DNA regulate nuclear rigidity. *MBoC*. **28**, 1580–1589 (2017).
16. K. N. Dahl, A. J. Engler, J. D. Pajerowski, D. E. Discher, Power-Law Rheology of Isolated Nuclei with Deformation Mapping of Nuclear Substructures. *Biophysical Journal*. **89**, 2855–2864 (2005).
17. C. M. Hobson, M. Kern, E. T. O'Brien, A. D. Stephens, M. R. Falvo, R. Superfine, Correlating nuclear morphology and external force with combined atomic force microscopy and light sheet imaging separates roles of chromatin and lamin A/C in nuclear mechanics. *MBoC*. **31**, 1788–1801 (2020).
18. A. Tajik, Y. Zhang, F. Wei, J. Sun, Q. Jia, W. Zhou, R. Singh, N. Khanna, A. S. Belmont, N. Wang, Transcription upregulation via force-induced direct stretching of chromatin. *Nature Mater*. **15**, 1287–1296 (2016).
19. A. H. B. de Vries, B. E. Krenn, R. van Driel, V. Subramaniam, J. S. Kanger, Direct observation of nanomechanical properties of chromatin in living cells. *Nano Lett*. **7**, 1424–1427 (2007).
20. Y. Shin, Y.-C. Chang, D. S. W. Lee, J. Berry, D. W. Sanders, P. Ronceray, N. S. Wingreen, M. Haataja, C. P. Brangwynne, Liquid Nuclear Condensates Mechanically Sense and Restructure the Genome. *Cell*. **175**, 1481-1491.e13 (2018).
21. C. M. Caragine, S. C. Haley, A. Zidovska, Nucleolar dynamics and interactions with nucleoplasm in living cells. *Elife*. **8**, e47533 (2019).
22. M. S. Syrchina, A. M. Shakhov, A. V. Aybush, V. A. Nadtochenko, "Optical trapping of nucleolus reveals viscoelastic properties of nucleoplasm inside mouse germinal vesicle oocytes" (preprint, Biophysics, 2020), , doi:10.1101/2020.03.19.999342.
23. M. Mittasch, A. W. Fritsch, M. Nestler, J. M. Iglesias-Artola, K. Subramanian, H. Petzold, M. Kar, A. Voigt, M. Kreysing, "Active gelation breaks time-reversal-symmetry of mitotic chromosome mechanics" (preprint, Biophysics, 2018), , doi:10.1101/296566.
24. B. Seelbinder, M. Jain, E. Erben, S. Klykov, I. D. Stoev, M. Kreysing, "Non-invasive Chromatin Deformation and Measurement of Differential Mechanical Properties in the Nucleus" (preprint, Cell Biology, 2021), , doi:10.1101/2021.12.15.472786.
25. C. Monzel, C. Vicario, J. Piehler, M. Coppey, M. Dahan, Magnetic control of cellular processes using biofunctional nanoparticles. *Chem Sci*. **8**, 7330–7338 (2017).

26. D. Liße, C. Monzel, C. Vicario, J. Manzi, I. Maurin, M. Coppey, J. Piehler, M. Dahan, Engineered Ferritin for Magnetogenetic Manipulation of Proteins and Organelles Inside Living Cells. *Adv. Mater.* **29**, 1700189 (2017).

27. S. M. Janicki, T. Tsukamoto, S. E. Salghetti, W. P. Tansey, R. Sachidanandam, K. V. Prasanth, T. Ried, Y. Shav-Tal, E. Bertrand, R. H. Singer, D. L. Spector, From silencing to gene expression: real-time analysis in single cells. *Cell*. **116**, 683–698 (2004).

28. T. Tsukamoto, N. Hashiguchi, S. M. Janicki, T. Tumbar, A. S. Belmont, D. L. Spector, Visualization of gene activity in living cells. *Nat Cell Biol*. **2**, 871–878 (2000).

29. X. Darzacq, Y. Shav-Tal, V. de Turris, Y. Brody, S. M. Shenoy, R. D. Phair, R. H. Singer, In vivo dynamics of RNA polymerase II transcription. *Nat Struct Mol Biol*. **14**, 796–806 (2007).

30. L. Toraille, K. Aïzel, É. Balloul, C. Vicario, C. Monzel, M. Coppey, E. Secret, J.-M. Siaugue, J. Sampaio, S. Rohart, N. Vernier, L. Bonnemay, T. Debuisschert, L. Rondin, J.-F. Roch, M. Dahan, Optical Magnetometry of Single Biocompatible Micromagnets for Quantitative Magnetogenetic and Magnetomechanical Assays. *Nano Lett.* **18**, 7635–7641 (2018).

31. M. Bongaerts, K. Aizel, E. Secret, A. Jan, T. Nahar, F. Raudzus, S. Neumann, N. Telling, R. Heumann, J.-M. Siaugue, C. Ménager, J. Fresnais, C. Villard, A. El Haj, J. Piehler, M. A. Gates, M. Coppey, Parallelized Manipulation of Adherent Living Cells by Magnetic Nanoparticles-Mediated Forces. *IJMS*. **21**, 6560 (2020).

32. M. Ganji, I. A. Shaltiel, S. Bisht, E. Kim, A. Kalichava, C. H. Haering, C. Dekker, Real-time imaging of DNA loop extrusion by condensin. *Science*. **360**, 102–105 (2018).

33. E. A. Galburt, S. W. Grill, C. Bustamante, Single molecule transcription elongation. *Methods*. **48**, 323–332 (2009).

34. P. E. Rouse, A Theory of the Linear Viscoelastic Properties of Dilute Solutions of Coiling Polymers. *The Journal of Chemical Physics*. **21**, 1272–1280 (1953).

35. B. Gu, T. Swigut, A. Spencley, M. R. Bauer, M. Chung, T. Meyer, J. Wysocka, Transcription-coupled changes in nuclear mobility of mammalian cis-regulatory elements. *Science*. **359**, 1050–1055 (2018).

36. J. Li, A. Dong, K. Saydaminova, H. Chang, G. Wang, H. Ochiai, T. Yamamoto, A. Pertsinidis, Single-Molecule Nanoscopy Elucidates RNA Polymerase II Transcription at Single Genes in Live Cells. *Cell*. **178**, 491-506.e28 (2019).

37. H. Hajjoul, J. Mathon, H. Ranchon, I. Goiffon, J. Mozziconacci, B. Albert, P. Carrivain, J.-M. Victor, O. Gadal, K. Bystricky, A. Bancaud, High-throughput chromatin motion tracking in living yeast reveals the flexibility of the fiber throughout the genome. *Genome Res.* **23**, 1829–1838 (2013).

38. I. Solovei, A. S. Wang, K. Thanisch, C. S. Schmidt, S. Krebs, M. Zwerger, T. V. Cohen, D. Devys, R. Foisner, L. Peichl, H. Herrmann, H. Blum, D. Engelkamp, C. L. Stewart, H. Leonhardt, B. Joffe, LBR and Lamin A/C Sequentially Tether Peripheral Heterochromatin and Inversely Regulate Differentiation. *Cell*. **152**, 584–598 (2013).

39. C.-H. Chuang, A. E. Carpenter, B. Fuchsova, T. Johnson, P. de Lanerolle, A. S. Belmont, Long-Range Directional Movement of an Interphase Chromosome Site. *Current Biology*. **16**, 825–831 (2006).

40. N. Khanna, Y. Hu, A. S. Belmont, HSP70 Transgene Directed Motion to Nuclear Speckles Facilitates Heat Shock Activation. *Current Biology*. **24**, 1138–1144 (2014).

41. S. Leidescher, J. Ribisel, S. Ullrich, Y. Feodorova, E. Hildebrand, A. Galitsyna, S. Bultmann, S. Link, K. Thanisch, C. Mulholland, J. Dekker, H. Leonhardt, L. Mirny, I. Solovei, Spatial organization of transcribed eukaryotic genes. *Nat Cell Biol*. **24**, 327–339 (2022).

42. C. P. Caridi, C. D'Agostino, T. Ryu, G. Zapotoczny, L. Delabaere, X. Li, V. Y. Khodaverdian, N. Amaral, E. Lin, A. R. Rau, I. Chiolo, Nuclear F-actin and myosins drive relocalization of heterochromatic breaks. *Nature*. **559**, 54–60 (2018).

43. V. I. P. Keizer, S. Grosse-Holz, M. Woringer, L. Zambon, K. Aizel, M. Bongaerts, F. Delille, L. Kolar-Znika, V. F. Scolari, S. Hoffmann, E. J. Banigan, L. A. Mirny, M. Dahan, D. Fachinetti, A. Coulon, Data, software and documentation for "Live-cell micromanipulation of a genomic locus reveals interphase chromatin mechanics" (2022), , doi:10.5281/zenodo.4626942.

44. M. Green, A. Thorburn, R. Kern, P. M. Loewenstein, The use of cell microinjection for the in vivo analysis of viral transcriptional regulatory protein domains. *Methods Mol Med*. **131**, 157–186 (2007).

45. A. Edelstein, N. Amodaj, K. Hoover, R. Vale, N. Stuurman, Computer Control of Microscopes Using μManager. *Current Protocols in Molecular Biology*. **92** (2010), doi:10.1002/0471142727.mb1420s92.

46. J. M. D. Coey, *Magnetism and magnetic materials* (Cambridge University Press, Cambridge, 2010).

47. S. C. Weber, J. A. Theriot, A. J. Spakowitz, Subdiffusive motion of a polymer composed of subdiffusive monomers. *Phys. Rev. E*. **82**, 011913 (2010).

48. B. van Steensel, A. S. Belmont, Lamina-Associated Domains: Links with Chromosome Architecture, Heterochromatin, and Gene Repression. *Cell*. **169**, 780–791 (2017).

49. F. Höfling, T. Franosch, Anomalous transport in the crowded world of biological cells. *Rep. Prog. Phys.* **76**, 046602 (2013).

Acknowledgments: We dedicate this work to the memory of Maxime Dahan, who died in July 2018. The authors would like to acknowledge scientific inputs from: C. Giovannangeli and J.-P. Concordet (MNHN), T. Pons and N. Lequeux (ESPCI), M. Coppey (Institut Curie), Marco Cosentino Lagomarsino (IFOM), and

the members of the Coulon and Fachinetti teams. We acknowledge the current and past members of the Dahan/Coppey/Hajj team and UMR168, including C. Monzel, D. Liße, J. Manzi, E. Baloul, C. Vicario and D. Normanno, for their earlier work and technical help on nanoparticles and microinjection, and E. Secret and A. Michel-Tourgis (UMR8234 CNRS) for help with magnetic nanoparticle characterization. The authors acknowledge the Flow Cytometry Core Facility of the Institut Curie, the BMBC platform of UMR168, the machine shop of UMR168, the technological platform of the Institut Pierre-Gilles de Gennes (IPGG) for access to microfabrication facilities, the PICT-IBiSA@Pasteur Imaging Facility of the Institut Curie (member of the France Bioimaging National Infrastructure; ANR-10-INBS-04), and the MPBT platform (Physical Measurements at Low Temperatures) of Sorbonne Université.

Funding: This work received funding from:

- the LabEx CELL(N)SCALE (ANR-11-LABX-0038, ANR-10-IDEX-0001-02) (MD, DF, AC)
- the Agence Nationale de la Recherche (project CHROMAG, ANR-18-CE12-0023-01) (MD, AC),
- the PRESTIGE program of Campus France (PRESTIGE-2018-1-0023) (VK)
- the ATIP-Avenir program of CNRS and INSERM, the Plan Cancer of the French ministry for research and health (AC, DF),
- the European Research Council (ERC) under the European Union's Horizon 2020 research and innovation program (grant agreement No 757956) (AC),
- the LabEx DEEP (ANR-11-LABX-0044, ANR-10-IDEX-0001-02) (AC),
- the program Fondation ARC (grant agreement PJA 20161204869) (AC)
- the Institut Curie (DF, AC)
- the Centre National de la Recherche Scientifique (CNRS) (AC, DF)
- the European Union's Horizon 2020 research and innovation program under the Marie Skłodowska-Curie grant agreement No 666003 (SH)
- the NIH GM114190 grant (LAM),
- the MIT-France Seed Fund (LAM, MD),
- LAM is a recipient of Chaire Blaise Pascal by Île-de-France Administration (LAM).

Author contributions: MD, DF and AC conceptualized the project. MD, DF, VIPK and AC obtained funding. VIPK, MD, DF and AC designed the experiments. VIPK, LZ, FD and AC obtained the data. VIPK, LZ, KA, MB, FD, LKZ, SH produced reagents and provided key technical expertise. MW, VIPK and AC preformed image analysis. MW, VIPK, SGH, VFS and AC analyzed trajectories. SGH, EJB and LAM preformed polymer modeling. VIPK, SGH, MW, VFS, EJB, LAM, DF and AC interpreted the results. DF and AC supervised the experimental work. AC supervised the image analysis work. EJB and LAM supervised the modeling work. AC drafted the manuscript with inputs from VIPK, MW, DF, SGH, EJB and LAM. All authors participated in reviewing and editing the manuscript.

Competing interests: The authors declare that they have no competing interests. KA is currently employed by TreeFrog Therapeutic as Research & Development engineer in encapsulation technologies.

Data and materials availability: Cell line and plasmids are available upon request. All data and codes are available through GitHub and Zenodo (*43*), as summarized in table S2.

Supplementary Materials

Materials and Methods

Supplementary Text

Figs. S1 to S12

Tables S1 and S2

Movies S1 to S4